PCCP

Accepted Manuscript

ROYAL SOCIETY OF CHEMISTRY

www.rsc.org/pccp

www.rsc.org/pccp FULL ARTICLE

A Novel Ni-WC/AC Catalyst with Enhanced Electroactivity for Glucose Oxidation

Suitao Qi*, Jiaqi Yue, Chen Hao, Yingying Li, Chunhai Yi and Bolun Yang

WC-doped Ni over active carbon catalyst (Ni-WC/AC) prepared by incipient wetness impregnation, is proposed as an anode for the amplified electrochemical oxidation of glucose in 0.1 M KOH solution. Cyclic voltammetry and morphology characterizations were used to explore these electrocatalysts. It was found that Ni-WC/AC catalysts were nanoparticles with diameter of 10 nm and the 20%wtNi-20%wtWC/AC catalyst showed a superior electrocatalytic activity toward glucose oxidation. The extraordinary activity obtained at 20%wtNi-20%wtWC/AC modified glass carbon electrode (GCE) is attributed to the synergistic effect between Ni and WC toward the glucose electroxidation.

Key word: Ni-WC, glucose, electroxidation catalysis

Introduction

Electrocatalytic oxidation of glucose has gained much attention due to its important applications in many fields such as biotechnology, clinical diagnostics, and food industry [1-3]. Numerous efforts were devoted to selecting noble metals and their alloys such as Pt [4], Au [5-7], Pt-Au [8], Pt-Pd [9] and Au-Ag [10] for glucose oxidation. Although the noble metal electrode exhibited the high elecrocatalytic activity towards directly oxidation of glucose, its surface was easily fouled by the chemisorbed intermediates or the adsorbed chloride ions, which would result in the poor operational stability of electrodes. In addition, the high price of noble metal may limit its commercial application. This has turned the recent efforts to the development of relatively cheap materials, such as Ni [11-13], NiO [14-16], $Ni(OH)_2$ [17,18], Cu [19], Ru(Ⅲ) [20], $LaTiO_3$-$Ag_{0.2}$ [21] and FeOOH [22]. As Nickel and nickel hydroxide exhibited the excellent catalytic performance in alkaline medium for glucose oxidation, Ni based materials such as Ni-Cu [23], Ni-Pt [24], Ni-Pd [25], NiOx-MnOx [26] and $Ni(OH)_2$-$Co(OH)_2$ [27] were extensively investigated among these catalysts materials.

On the other hand, since Levy and Boudart [28] firstly reported that the transition metal carbide WC is similar to Pt in the electronic structure and catalytic properties, it has been regarded as the promising candidate material owe to its Pt-like catalytic activity, excellent stability, high resistance oxidation and CO poisoning. There are some reports that WC has shown great electrocatalytic activity for methanol oxidation. To the best of our knowledge, WC acted as a catalyst for electrocatalytic oxidation of glucose has not been reported. Active porous carbon could facilitate the mass transport in the electrodes compared with some other carbon materials. Hence, it would be interesting thing to combine Ni with WC supported on active carbon to exploit their combined characteristics toward glucose electroxidation.

In this work, a series of compound WC-doped Ni over active carbon (Ni-WC/AC) catalysts with the certain content of Ni were prepared by incipient wetness impregnation and tested as an electrocatalyst toward glucose electroxidation. It exhibited the high stability and the remarkable electrocatalytic activity for glucose oxidation, revealing the feasibility to use Ni-WC as a highly active, durable, and cost-effective electrocatalyst in nonenzymatic glucose sensor or glucose fuel cell.

Experimental

The compound eletrocatalysts Ni-WC/AC and WC/AC were prepared by incipient wetness impregnation in temperature program method. The complete details of preparation process were described in our previous work [29].

The electrochemical measurements (Cyclic voltammetry) were performed using a conventional three-electrode system with a platinum wire as the auxiliary electrode and an Hg|HgO (1.0 M KOH) as the reference in a CHI 760 electrochemical workstation (CH Instrument, China). The working electrode was the modified glassy carbon electrode (GCE). The modification of GCE by means of the combination of Ni with WC was achieved by the following steps. A certain amount of WC/AC or Ni-WC/AC was added to the prepared mixture of 30 μL Nafion (Nf), 20 μL H_2O and 2.5 mL ethanol, and then the mixture were dispersed with the mild ultrasonication for 30 min in order to form a homogeneous liquid. Whereafter, 5 μL of the homogeneous liquid was dropped onto a glassy carbon electrode (d = 3 mm) and allowed to dry in ambient air for 24 h. The modified Ni-WC/AC/GCE was obtained. GCE was precleaned by polishing with 1.0, 0.3, and 0.05 μm alumina slurries, followed with sonication in ethanol and water successively.

The crystal structure of the sample was characterized using X-ray diffraction equipment (XRD, Holland PANalytica X'Pert ProX) using a Cu Kα radiation. The catalyst surface morphology were observed by field emission scanning electron microscope (FE-SEM) coupled with energy dispersive spectrometer (EDS) (sirion200,U.S.) and transmission electron microscope (TEM) with selected area electron diffraction (JEM-2100, Japan). The surface composition of the samples was characterized by X-ray photoemission spectroscopy (XPS, Kratos AXIS Ultra).

Results and discussion

3.1 Characterization of Ni-WC/AC catalyst

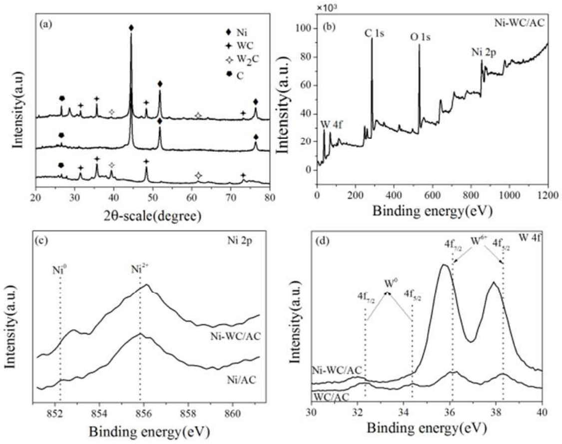

Fig.1 (a) XRD patterns of 20%wtNi-20%wtWC/AC, 20%wtNi/AC and 20%wtWC/AC; XPS spectra of (b) 20%wtNi-20%wtWC/AC (c) Ni 2p and (d) W 4f of 20%wtNi-20%wtWC/AC, 20%wtNi/AC and 20%wtWC/AC.

As shown in Fig. 1a, the diffraction peaks consistent with C, WC and Ni can be found in the XRD patterns of 20%wtNi-20%wtWC/AC. The diffraction peaks of 20%wtNi-20%wtWC/AC at 2θ = 44.42, 51.78, and 76.36 are consistent with the (111), (200), (220) planes of the cubic structure of Ni (JCPDS No.01-070-1849), demonstrating that the major composition is metallic Ni. Similarly, the diffraction peaks of 20%wtNi-20%wtWC/AC at 2θ = 31.60, 35.72, 48.26 and 73.38 are consistent with the (001), (100), (101) and (111) planes of the hexagonal structure of WC (JCPDS No.03-065-8828), while the diffraction peaks at 2θ =39.45, 61.77 are in accordance with the W_2C (121) and (023) (JCPDS No.03-065-8829). The XRD diffractions of WC indicated that the formed carbides mainly were WC including a few W_2C. The intensity of W_2C diffraction peaks was reduced in Ni-WC/AC patterns, which may due to the following calcinations process of catalysts preparation. Accordingly, it can be concluded that the nanoparticles prepared in this work include nickel of face-centered cubic (fcc) structure and tungsten carbide of hexagonal-close packed (hcp) structure as major phases.

To explore the interaction between Ni and WC, the chemical states of the catalysts surface are analyzed by X-ray photoelectron spectrum (XPS). As shown in Fig. 1b, the survey XPS spectra display a set of peaks corresponding with C 1s, O 1s, W 4f and Ni 2p spectra, respectively, which is in accordance with the XRD results. It should be noted that C 1s (284.8eV) is ascribed to an active carbon substrate and WC, and the peak at 532.2eV is attributed to O 1s spectra. The existence of oxygen might be the adsorbed oxygen on the catalyst surface or nickel oxide. As shown in Fig. 1c, the Ni 2p spectrum of Ni/AC shows two peaks with Ni 2p3/2 binding energy of 852.2 eV and 855.8 eV, which is characteristic of Ni^0 [31] and Ni^{2+} [32], respectively. Compared with Ni/AC, the Ni 2p spectrum of Ni-WC/AC positively shifts (852.8 eV and 856.2 eV), which is attributed to the electron transfer effect from Ni to WC metal [33]. The W 4f spectrum of WC/AC (Fig. 1d) shows that both W^0 (W $4f_{5/2}$ binding energy of 34.3 eV and W $4f_{7/2}$ binding energy of 32.3 eV) and W^{6+} (W $4f_{5/2}$ binding energy of 38.3 eV and W $4f_{7/2}$ binding energy of 36.1 eV) [34] appear on the WC/AC surface. In contrast to the positive shift of Ni 2p, the W 4f binding energy of Ni-WC/AC shifts negatively relative to that of WC/AC. In conclusion, the positive shift of Ni 2p binding energy and the negative shift of W 4f binding energy for Ni-WC/AC can testify to the electron interaction existing between Ni and WC, and this synergistic effect between metal and support can significantly improve the performance of the electrocatalyst [35].

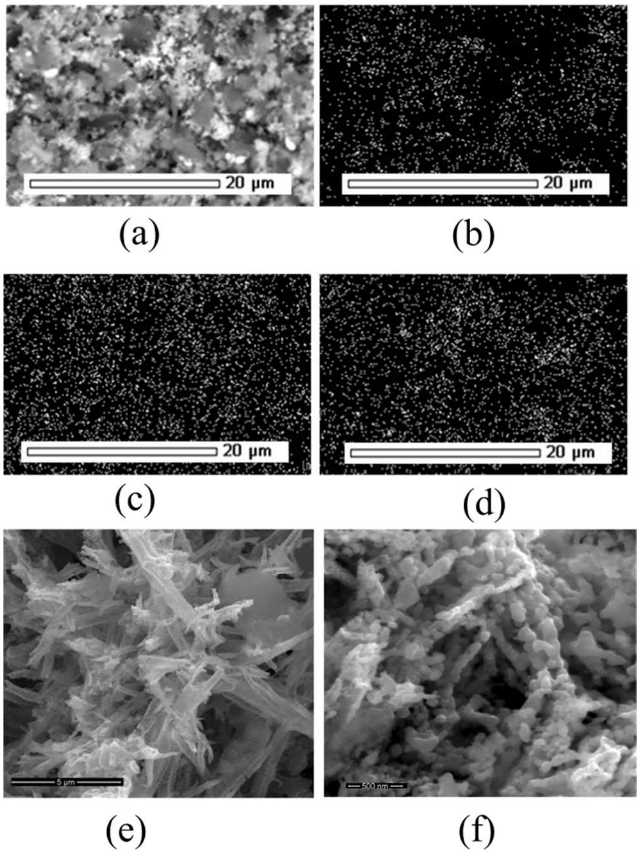

(a) (b)

(c) (d)

(e) (f)

Fig. 2 (a, e, f) SEM images of 20%wtNi-20%wtWC/AC at different magnifications, (b-d) elemental mapping of C, Ni and W

Fig. 2a shows the scanning electron microscopy (SEM) image of 20%wtNi-20%wtWC/AC. Fig. 2b-d shows the elements mapping of C, Ni and W. Clearly, it can be found that Ni and W are well distributed throughout the catalyst. The uniform distribution of Ni and W suggests the uniform coverage of Ni and WC around the substrate of active carbon. Seen from the SEM images in Fig. 2e and Fig. 2f, these catalysts displayed as some staggered rods with a diameter of 300nm or so, which are formed by many interconnected small particles.

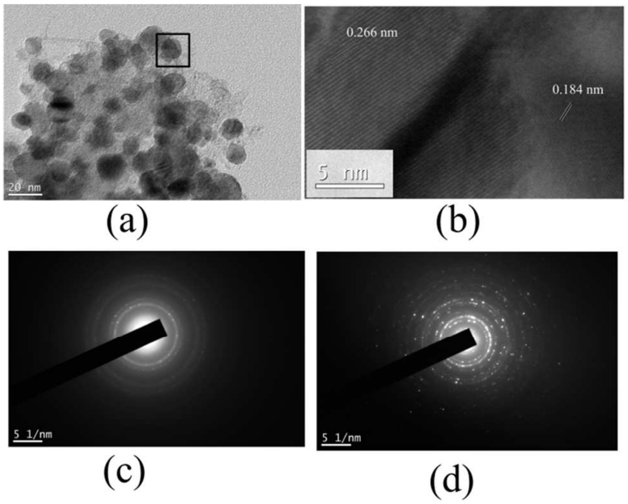

Fig. 3. (a) TEM image of 20%wtNi-20%wtWC/AC; (b) HRTEM image of 20%wtNi-20%wtWC/AC. SAED pattern of (c)20%wtNi/AC and (d)20%wtNi-20%wtWC/AC.

Fig. 3a shows TEM micrograph of 20%wtNi-20%wtWC/AC catalyst, where a mass of nanoparticles are clearly observed and the nanoparticles have a diameter of 10nm. The measured lattice spacing of 0.184Å and 0.266Å corresponded to the Ni (200) and WC (001) was shown in Fig.3b and the junction of the two lattice fringes reveals that Ni is on the top of WC. In addition, both SAED patterns of 20%wtNi-20%wtWC/AC and 20%wtNi/AC nanoparticals exhibits the well-ordered rings (Fig. 3c-d), indicating that both of them are polycrystalline. Compared to 20%wtNi/AC catalyst, the extra rings for SAED patterns of 20%wtNi-20%wtWC/AC would be attributed to WC.

Table 1. EDS results of different Ni-WC/AC catalyst surfaces

Catalyst	Element/Mass%		
	Ni	W	C
10%wtNi-20%wtWC/AC	11.63	14.06	74.31
20%wtNi-20%wtWC/AC	21.12	17.27	61.61
30%wtNi-20%wtWC/AC	39.25	13.62	47.13

The EDS results of catalysts with the different Ni or WC content were listed in Table 1. The surface compositions of catalysts, except for 30%wtNi-20%wtWC/AC, are basically consistent with that of the bulk phase, revealing that active elements disperse evenly on both the surface and the bulk. The higher Ni content may be due to that Ni unevenly disperses for 30%wtNi-20%wtWC/AC catalyst. In addition, it must be pointed out that some of C was attributed to the substrate AC.

3.2 Electrocatalytic oxidation of glucose at the modified electrodes

The electrocatalytic behaviours of the modified electrodes towards glucose oxidation in an alkaline medium were tested by cyclic voltammetry (CV). Fig. 4 shows the CVs of the 20%wtWC/AC/GCE in the absence and the presence of 1.0mM glucose in 0.1M KOH solution. No redox peaks were observed, which indicated that 20%wtWC/AC/GCE has no current response towards glucose.

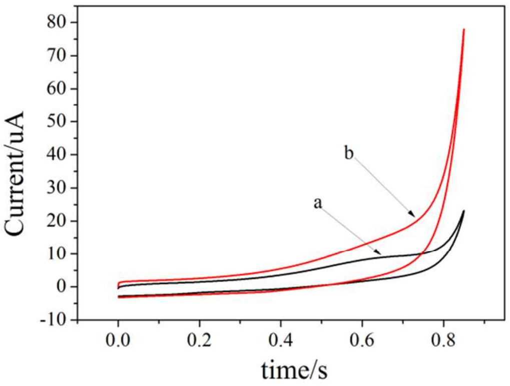

Fig. 4. Cyclic voltammograms of 20%wtWC/AC in the absence(a) and presence(b) of 1mM glucose in 0.1 M KOH solution. Scan rate: 50 mV s^{-1}. 25℃.

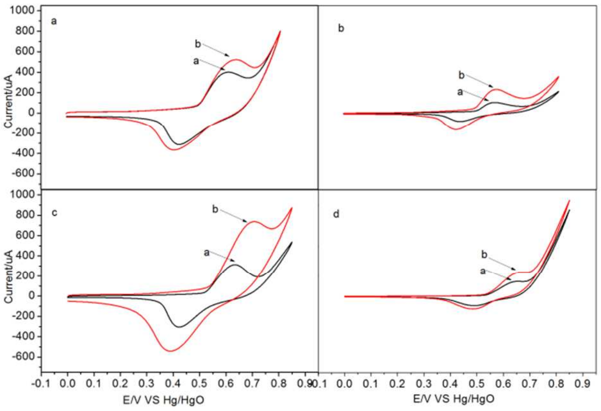

Fig. 5. Cyclic voltammograms of (a) 20%wtNi/AC (b)10%wtNi-20%wtWC/AC (c) 20%wtNi-20%wtWC/AC (d) 30%wtNi-20%wtWC/AC in 0.1 M KOH solution with and without 1mM glucose. Curve a is the CV response in 0.1 M KOH solution and curve b is the response in 0.1 M KOH solution containing 1mM glucose. Scan rate: 50 mV/s, 25℃.

Fig.5a shows the CVs of the 20%wtNi/AC/GCE in the absence and the presence of 1.0 mM glucose in 0.1 M KOH solution. The blank experiment test of Ni/AC/GCE presents a pair of redox peaks with the peak potentials located at 0.63 V and 0.38 V (curve a, Fig. 5a), which is assigned to the Ni^{3+}/Ni^{2+} redox couple[30]. The addition of 1.0 mM glucose made the anodic current significantly increased (curve b, Fig.5a), indicating that the 20%wtNi/AC/GCE exhibits the stronger electrocatalytic activity toward glucose oxidation compared to 20%wtWC/AC. Compared to that at 20%wtNi/AC/GCE, the response obtained at 20%wtNi-20%wtWC/AC/GEC slightly decreases in 0.1 M KOH (curve a, Fig.5c). This may be due to some Ni active sites covered by WC. However the peak current at 20%wtNi-20%wtWC/AC/GEC is higher than that at 20%wtNi/AC/GEC in 0.1 M KOH solution containing 1 mM glucose (curve b, Fig.5c). The enhanced electrocatalyst activity of 20%wtNi-20%wtWC/AC would benefit from the synergistic effect between Ni and WC toward glucose electroxidation. It has been found that doping Ni with WC indeed changes the electron distribution of Ni atom in our previous work [29] and there are resonance between

Ni 2p orbit and W 4f orbit, which is in accordance with the XPS results.

It is noteworthy to mention that the electrocatalytic activities of Ni-WC/AC/GEC could be correlated with the different Ni content. As shown in Fig.5b, 5c and 5d, a weak response was observed at the 10%wtNi-20%wtWC/AC/GCE revealed that Ni active sites is limited on the electrode surface. With the increase of Ni from 10%wt to 30%wt, the corresponding current passes through a maximum at 20%wtNi-20%wtWC/AC/GCE, which indicated that the formation of synergistic effect required a proper ratio of Ni and WC.

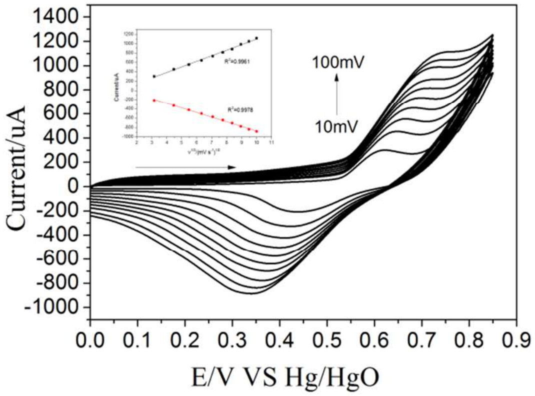

Fig.6. CVs of 20%wtNi-20%wtWC/AC for 1.0mM glucose in 0.1 M KOH at various scan rates: 10, 20, 30, 40,50, 60, 70, 80, 90,100 mV/s. The inset presents the plots of peak current vs. $v^{1/2}$.

Fig. 6 presents the CVs at the 20%wtNi-20%wtWC/AC/GCE for 1.0 mM glucose in 0.1 M KOH with the various scan rate ranging from 10 to 100 mV/s. Both the anodic and cathodic peak currents from CV were linearly correlated to the square root of scan rate (the inset of Fig. 4), which demonstrated that the glucose electroxidation is a typical diffusion-controlled process, which can be used to guide the experiment process.

3.3 Amperomertic responses of 20%wtNi-20%wtWC/AC/GEC to glucose

Fig. 7a exhibits the amperometric response to glucose on the 20%wtNi-20%wtWC/AC/GCE, which was evaluated by measuring the current response at a fixed potential with adding the glucose amount. A well-defined, stable and fast amperometric responses could be observed at +0.65 V with the successive addition of glucose into 0.1 M KOH aqueous solution. It shows a linear dependence (R = 0.944) in the glucose concentration range of 0.1 mM to 7.5 mM with a sensitivity of 20.88 uA/mM (Fig. 7b). The detection limit of the 20%wtNi-20%wtWC/AC/GCE is 5 uM.

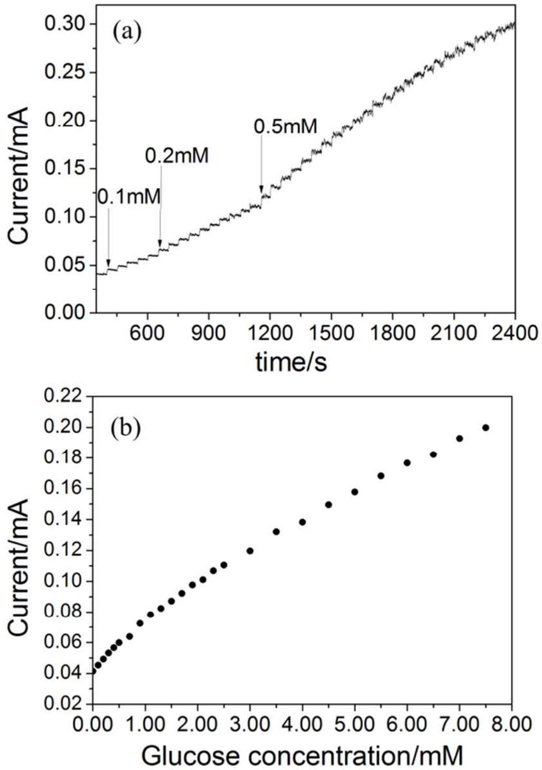

Fig. 7. (a) Current–time curves of the 20%wtNi-20%wtWC/AC/GCE at +0.65 V with successive addition of 0.1, 0.2 and 0.5 mM glucose in 0.1 M KOH. (b) The calibration curves obtained from the current–time curves in (a).

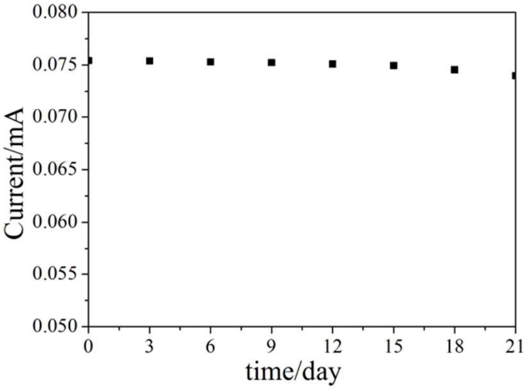

Fig. 8. Long-term stability of 20%wtNi-20%wtWC/AC toward glucose oxidation over 3 weeks in 0.1 M KOH solution at +0.65 V with addition of 1.0mM glucose.

The stability test of the 20%wtNi-20%wtWC/AC/GCE was also conducted by discontinuously measurements every 3 days and the results were shown in Fig.8. It was found that even if the electrode was stored for three weeks at ambient conditions, it could remain 98% of its original response exhibiting the good stability.

Conclusions

A modified Ni-WC/AC/GCE was prepared and tested the electrocatalytic activity toward glucose oxidation in alkaline media. It was found that Ni-WC/AC/GCE exhibited the remarkable current response. In addition, it was found that direct electrochemical response of glucose at the Ni-WC/AC/GCE was gradually improved with increased glucose concentration in 0.1M KOH solution. It is important to highlight that 20%wtNi-20%wtWC/AC exhibits the enhanced electrocatalytic activity toward glucose oxidation, which is attributed to the synergistic effect between Ni and WC.

Acknowledgement

Financial support for this work from the National Natural Science Foundation of China (21006076) and State Key Laboratory of Multiphase Flow in Power Engineering are gratefully acknowledged.

Notes and references

State Key Laboratory of Multiphase Flow in Power Engineering, xi'an Jiaotong University, 28 Xianning West Road, Xi'an Shaanxi, P.R.China. Tel: +8615809201586; E-mail: suitaoqi@mail.xjtu.edu.cn.

1 L. Li, K. Scott and E. H. Yu, *Journal of Power Sources*, 2013, 221, 1-5.
2. Y. Liu, H. Teng, H. Q. Hou and T. Y. You, *Biosensors and Bioelectronics*, 2009, 24, 3329–3334.
3. S. B. Aoun, G. S. Bang, T. Koga, Y. Nonaka, T. Sotomura and I. Taniguchi, *Electrochemistry Communications*, 2003, 5, 317–320.
4. S. Park, T. D. Chung and H. C. Kim, *Anal. Chem.*, 2003, 75, 3046-3049.
5. M. Tominaga, T. Shimazoe, M. Nagashima and I. Taniguchi, *Electrochemistry Communications*, 2005, 7, 189–193.
6. N. Arjona, M. Guerra-Balcázar, G. Trejo, J. Ledesma-Garcı´ and L. G. Arriaga, *New Journal of Chemistry*, 2012, 36, 2555–2561.
7. M. Pasta, L. B. Hu, F. La Mantia and Y. Cui, *Electrochemistry Communications*, 2012, 19, 81–84.
8. J. Ryu, K. Kim, H. S. Kim, H. Thomas Hahn and D. Lashmore, *Biosensors and Bioelectronics*, 2010, 26, 602–607.
9. Y. Bai, Y. Y. Sun and C. Q. Sun, *Biosensors and Bioelectronics*, 2008, 24, 579–585.
10 M. Tominaga, T. Shimazoe, M. Nagashima, H. Kusuda, A. Kubo, Y. Kuwahara and I. Taniguchi, *Journal of Electroanalytical Chemistry*, 2006, 590, 37–46.
11 L. M. Lu, L. Zhang, F. L. Qu, H. X. Lu, X. B. Zhang, Z. S.Wu, S. Y. Huan, Q. A. Wang, G. L. Shen and R. Q. Yu, *Biosensors and Bioelectronics*, 2009, 25, 218–223
12 C. Z. Zhao, C. L. Shao, M. H. Li and K. Jiao, *Talanta*, 2007, 71, 1769–1773.
13 R.M. Abdel Hameed, Biosensors and Bioelectronics, 2013, 47, 248–257.
14 C. C. Li, Y. L. Liu, L. M. Li, Z. F. Du, S. J. Xu, M. Zhang, X. M. Yin and T. H. Wang, *Talanta*, 2008, 77, 455–459.
15 F. Cao, S. Guo, H. Y. Ma, D. C. Shan, S. X. Yang and J. Gong, *Biosensors and Bioelectronics*, 2011, 26, 2756–2760.
16 Y. Mu, D. L. Jia, Y. Y. He, Y. Q. Miao and H. L. Wu, *Biosensors and Bioelectronics*, 2011, 26, 2948–2952.
17 Y. M. Jiang, S. J. Yu, J. J. Li, L. P. Jia and C. M. Wang, *Carbon*, 2013, 63, 367-375.
18 Z. J. Luo, S. Yin, K. Wang, H. M. Li, L. G. Wang, H. Xu and J. X. Xia, *Materials Chemistry and Physics*, 2012, 132, 387– 394.
19 Z. J. Fan, B. Liu, X. H. Liu, Z. P. Li, H. G. Wang, S. R. Yang and J. Q. Wang, *Electrochimica Acta*, 2013,109, 602– 608.
20 A. K. Singh, S. Srivastava, J. Srivastava, R. Srivastava and P. Singh, *Journal of Molecular Catalysis A: Chemical*, 2007, 278, 72–81.
21 Y. Z. Wang, H. Zhong, X. M. Li, F. F. Jia, Y. X. Shi, W. G. Zhang, Z. P. Cheng, L. L. Zhang and J. K. Wang, *Biosensors and Bioelectronics*, 2013, 48, 56–60.
22 C. Xia and W. Ning, *Electrochemistry Communications*, 2010, 12, 1581–1584.
23 R. Qiu, X. L. Zhang, R. Qiao, Y. Li, Y. Kim, and Y. S. Kang, *Chem. Mater.*, 2007, 19, 4174-4180.
24 S. Kerzenmacher, M. Schroeder, R. Brämer, R. Zengerle and F. von Stetten, *Journal of Power Sources*, 2010, 195, 6516–6523.
25 F. J. Miao, B. R. Tao, L. Sun, T. Liu, J. C. You, L. W. Wang and P. K. Chu, *Sensors and Actuators B*, 2009, 141, 338–342.
26 S. M. El-Refaei, M. M. Saleh and M. I. Awad, *Journal of Power Sources*, 2013, 223, 125-128.
27 M. Vidotti, C. V. Greco, E. A. Ponzio and S. I. C. D. Torresi, *Electrochemistry Communications*, 2006, 8, 554–560.
28 R. B. Levy and M. Boudart, *Science*, 1973, 181, 547-549.
29 S. T. Qi, J. Q. Yue, Y. Y. Li, H. Jun, C. H.Yi and B. L. Yang, *Catal. Lett.*, 2014, 144, 1443-9.
30 Q. D. Wu, X. P. Gao, G. R. Li, G. L. Pan, T. Y. Yan and H. Y. Zhu, *J Phys Chem C*, 2007, 111, 17082–17087.
31 V. V. Kaichev, A.Yu. Gladky, I. P. Prosvirin, A. A. Saraev, M. Hävecker, A. Knop-Gericke, R. Schlögl and V. I. Bukhtiyarov, *Surface Science*, 2013, 609, 113–118.
32 J. W. Zhao, Y. P. Song, P. T. Ma, J. P. Wang and J. Y. Niu, *J Solid State Chem*, 2009, 182, 1798-1805.
33 J. Yang, Y. Xie, R. Wang, B. Jiang, C. Tian, G. Mu, J. Yin, B. Wang and H. Fu, *ACS Appl. Mater. Interfaces*, 2013, 5, 6571-6579.
34 P. N. Ross and P. Stonehart, *Journal of catalysis*, 1975, 39, 298-301.
35 L. G. Feng, X. J.Sun, C. P. Liu, W. Xing, *Chem. Commun.*, 2012, 48, 419-421.